Electronic Supplementary Material (ESI) for ChemComm.

Electronic Supplementary Information

Uranium Capture Strategy based on Self-assembly in Hydroxyl-functionalized Ionic Liquids Extraction System

Baihua Chen,[a] Kaige Wu,[b] Yanqiu Yang,[a] Ning Wang,[a] Yi Liu,[a] Shuanglin Hu,[a] Jing Wang,[a] Jun Wen,[a] Sheng Hu,[a] Qingde Chen,[b] Xinghai Shen,*[b] and Shuming Peng*[a]

[a] Institute of Nuclear Physics and Chemistry, China Academy of Engineering Physics, Mianyang 621999, P. R. China

[b] Beijing National Laboratory for Molecular Sciences (BNLMS), Fundamental Science on Radiochemistry and Radiation Chemistry Laboratory, Center for Applied Physics and Technology, College of Chemistry and Molecular Engineering, Peking University, Beijing 100871, P. R. China

*Corresponding Authors: pengshuming@caep.cn (Shuming Peng), xshen@pku.edu.cn (Xinghai Shen)

Materials and Methods

Materials. Octyl(phenyl)-N,N-diisobutylcarbamoylmethylphosphine oxide (CMPO, 98%) was purchased from Carbosynth. Ionic liquids [HEMIm][NTf$_2$], [C$_1$C$_2$Im][NTf$_2$], [C$_1$C$_4$Im][NTf$_2$], [C$_1$C$_6$Im][NTf$_2$] and [C$_1$C$_8$Im][NTf$_2$], (purities>99%, structures shown in Scheme 1) were provided by Lanzhou Institute of Chemical Physics, Chinese Academy of Sciences. High purity $UO_2(NO_3)_2\cdot 6H_2O$ (99.9%) was obtained from Aladdin, China, dried for more than 48 h at 100 ^oC under vacuum condition, and stored in desiccator before use.

Synthesis of $UO_2(CMPO)_3(NO_3)_2$. $UO_2(NO_3)_2\cdot 6H_2O$ (402 mg, 0.8 mmol) was added to a solution of CMPO (978 mg, 2.4 mmol) in 1,2-dichloroethanein. The solution was stirred overnight at room temperature and then filtered to remove any insoluble compound. A yellow viscous liquid was obtained upon slow evaporation of 1,2-dichloroethanein. The compound was then dried overnight under high vacuum at 60 °C. The product was characterized by GC/MS and CHN analysis. GC/MS: m/z (+) 746.0. Elem. Anal. Calcd (%) for $C_{72}H_{126}N_5O_{14}P_3U$: C, 53.49; H, 7.86; N, 4.33. Found: C, 53.01; H, 7.88; N, 4.19.

Synthesis of $UO_2(CMPO)_3(NTf_2)_2$. $UO_2(NO_3)_2\cdot 6H_2O$ (1.53 g, 3 mmol), CMPO (3.67 g, 9 mmol) and 1,2-dichloroethanein were added sequentially to a 50 mL single-mouth flask. An aqueous solution of HNTf$_2$ (2.53 g, 9 mmol) was then added to the reaction and stirred overnight at room temperature. Afterwards, the organic layer was washed several times with ultra-pure water. A yellow viscous liquid was obtained upon slow evaporation of 1,2-dichloroethanein. The compound was then dried overnight under high vacuum at 60 °C. The product was characterized by GC/MS and CHN analysis. GC/MS: m/z (+) 746.0, 1772.1; m/z (-) 279.9. Elem. Anal. Calcd (%) for $C_{76}H_{126}F_{12}N_5O_{16}P_3S_4U$: C, 44.46; H, 6.19; N, 3.41. Found: C, 44.42; H, 6.23; N, 3.29.

Ionic liquid pretreatment. Ionic liquid [HEMIm][NTf$_2$] was equilibrated with HNO_3 solutions of certain concentrations for 24 h before use. The water content of the IL after treatment was determined to be ~101,000 ppm by standard Karl Fischer titration. Such HNO_3 solutions that had been equilibrated with [HEMIm][NTf$_2$] were later used for dissolving high purity $UO_2(NO_3)_2·6H_2O$.

CMPO solutions in ionic liquid. A stock solution of 0.4 mol/L ligand was prepared by dissolving CMPO with desired weight in $[HEMIm][NTf_2]$ using volumetric flask. Working solutions of lower ligand concentrations were prepared by quantitative dilution of the stock solution with $[HEMIm][NTf_2]$.

Uranium and other metal solutions. Uranium solutions for extraction experiments were prepared by dissolving weighted $UO_2(NO_3)_2·6H_2O$ in certain concentrations of HNO_3 solutions which had been equilibrated with $[HEMIm][NTf_2]$. The exact concentrations of uranium were determined by ICP-OES. Gold solution was prepared by dissolving desired amounts of $HAuCl_4·4H_2O$ (Sinopharm Chemical Reagent Co., Ltd. Beijing, China) in hydrochloric acid solution. Appropriate amounts of other metal chloride salts such as $CuCl_2·6H_2O$, $FeCl_3·6H_2O$, $MnCl_2·4H_2O$, $PbCl_2$, VCl_3, $ZnCl_2$ and $AlCl_3$, all procured from Kermel Chemical Reagent Co., Ltd. (Tianjin, China), were added to the hydrochloric acid, respectively, to prepare other metal solution. The HNO_3, $HClO_4$ and HCl were all of Optima grade from Fisher Scientific (Pittsburgh, PA, USA). All other reagents were of analytical grade and used as received. Milli-Q water with a resistivity great than 18 MΩ·cm was used in preparation of all the solutions.

Preparation of macroscopic SA sample. Equal volume of 5 mM $UO_2(NO_3)_2$ in 0.1 M HNO_3 and 30 mM CMPO in $[HEMIm][NTf_2]$ (balanced with 0.1 M HNO_3 overnight in advance) were mixed in a vial at 30 ^{o}C. A yellow SA sample appeared momentarily at the aqueous-IL interface. The mixture was left for one week without stirring and the size of the spherical SA sample gradually increased. The SA sample was then taken out with a tweezer and placed in a petri dish for air drying non-structural water and $[HEMIm][NTf_2]$ remaining on the surface.

Preparation of mesoscopic assembly. Solutions of 1 mM $UO_2(CMPO)_3(NTf_2)_2$ were prepared by dissolving proper amounts of $UO_2(CMPO)_3(NTf_2)_2$ in $[HEMIm][NTf_2]$ (dried overnight under high vacuum at 60 °C in advance). 150, 180, and 210 μL of ultrapure water, respectively, were added into a series of 3 mL solutions aforementioned. The solutions were vortexed and centrifuged immediately, as well as checked by dynamic light scatting (DLS) for the formation of mesoscopic assembly.

As a comparison, a series of 3 mL 1 mM $UO_2(CMPO)_3(NTf_2)_2$ in $[C_1C_2Im][NTf_2]$ solutions were added with 150, 180, and 210 μL of water respectively, and followed the same procedures as above.

Scanning Electron Microscope (SEM). The self-assembly sample was coated onto a silicon plate for SEM visualization. The morphology was examined by an analytical scanning electron microscope (SEM, Zeiss Uitra 55) with energy dispersive X-ray spectrometry (EDS) to provide the distribution of uranium, carbon, fluorine, oxygen, and sulphur elements.

Nuclear Magnetic Resonance (NMR) spectroscopy. ^{31}P NMR spectra of $UO_2(CMPO)_3(NO_3)_2$ and the self-assembly sample dissolved in deuterated dimethylsulfoxide (d_6-DMSO) were obtained on Bruker-500 MHz NMR (Bruker, Switzerland). ^{19}F NMR spectra of $[HEMIm][NTf_2]$ and the self-assembly sample were recorded by the same instrument accordingly.

Solid State Nuclear Magnetic Resonance (ss-NMR). The solid state NMR spectra were recorded with a JNM-ECZ600R spectrometer (JEOL) in single pulse with a tube diameter of 3.2 mm, mas frequency of 8 kHz and relaxation delay of 5 s. For ^{31}P and ^{19}F measurements, the resonant frequencies are 243 MHz and 564 MHz, respectively. The sampling time for all spectra is 1 h.

Mass Spectrometry (MS). The high-resolution mass spectrometry with electrospray ionization (ESI-HRMS) was performed on a Fourier transform ion cyclotron resonance mass spectrometer, Solarix XR (Bruker, Germany).

Fourier Transform Infrared Spectroscopy (FTIR). Infrared spectra were measured at room temperature on a Fourier transform infrared spectrometer (Nicolet is50, ThermoFisher).

Thermogravimetric Analyses (TGA). The thermogravimetric analysis (TGA) of the air-drying self-assembly sample was measured on Q600 TGA-DSC-DTA (Q600 SDT, TA) under N_2 atmosphere with the temperature ranging from room temperature to 600 ^{o}C at a heating rate of 10 $^{o}C/min$. The evolved gases were characterized and analyzed by online thermogravimetry/Fourier transform infrared spectrometry (TG/FTIR, PerkinElmer) under N_2 atmosphere with the temperature ranging from room temperature to 500 °C at a heating rate of 20 °C/min.

Elemental Analysis (EA). Elemental analysis was performed on an elemental analyzer (vario EL, Elementar Analysensysteme GmbH, Germany) with carbon, oxygen and hydrogen element contents measured.

Transmission Electron Microscope (TEM). A transmission electron microscope (TEM, Zeiss Libra 200) was used for viewing the morphology of the self-assembly sample that was grilled onto silicon plate.

Wide Angle X-ray Scattering (WAXS). The wide-angle X-ray scattering (WAXS) measurement was performed on the NANOSTAR instrument (Bruker AXS, Germany) with Microfocus Cu-Kα irradiation operating at 50 kV and 1 mA. The scattering intensity I(q) is measured as a function of scattering vector magnitude $q = 4\pi\sin\theta/\lambda$, where $\lambda = 0.154$ nm is the wavelength of the incident X-rays, and θ is half of the scattering angle. The detector was placed at 4.05 mm from the sample, resulting in a q range of 3.0-31 nm^{-1}. All data were corrected for absorption before background subtracting.

Dynamic Light Scatting (DLS). DLS measurements of mesoscopic assembly deriving from ILs added with different contents of water were performed on a Malvern Nano ZS90 instrument (Malvern Instruments, UK) at 30 °C and at a scattering angle of 90°. A He-Ne laser with a power of 4 mW was used as the light source.

Extraction experiment. Equal volume of CMPO in IL solution and uranium aqueous solution were mixed together in a glass sample vessel and left for a week at room temperature, as in **Preparation of macroscopic SA sample**. The detailed experimental conditions for investigating the effects of CMPO concentration in IL phase, HNO_3 concentration in aqueous phase and the reusability of IL were listed in table S2 and table S3 respectively.

The concentrations of uranium in the aqueous phase, IL phase and SA phase were determined by ICP-OES. The analytical sample of the IL phase was prepared as follows: 0.3 mL content of IL phase was repeatedly dried with a mixture of concentrated $HNO_3/HClO_4$ (10 mL, 2/1 by volume) in a glass flask for three times to destroy the organics. The flask was later heated slowly to 300 °C to vaporize excessive acids. 20

mL of 0.1 M HNO_3 was then added in the flask to dissolve uranium thoroughly for ICP-OES analysis. The procedure for the preparation of the SA phase analytical sample was almost the same, but with the total dissolution of the entire solid phase.

Calculations. The geometry structure of the complex formed by one UO_2^{2+} ion and three CMPO ligands were searched with the Gaussian 09 program.[1] The calculations were performed using the hybrid functional of B3LYP[2, 3] using the Becke's three-parameter functional and the correlation functional of Lee, Yang, and Parr(LYP), The small-core quasi relativistic pseudopotential ECP60MWB[4, 5] and the basis set of ECP60MWB_ANO[5, 6] from the Stuttgart/Cologne Group were used for U, and the polarized all-electron basis sets of 6-31G(d) were used for light atom C, H, O, N, and P. Several initial configurations including six-coordinated $UO_2(CMPO)_3^{2+}$ were tested, after geometry relaxation, the lowest energy configuration was in five-coordinated geometry, as presented in Figure S7. Of note, there are spaces for the complexes to overlap each other in the process of aggregation.

Reference

1 M. J. Frisch, G. W. Trucks, H. B. Schlegel, G. E. Scuseria, M. A. Robb, J. R. Cheeseman, G. Scalmani, V. Barone, B. Mennucci, G. A. Petersson, H. Nakatsuji, M. Caricato, X. Li, H. P. Hratchian, A. F. Izmaylov, J. Bloino, G. Zheng, J. L. Sonnenberg, M. Hada, M. Ehara, K. Toyota, R. Fukuda, J. Hasegawa, M. Ishida, T. Nakajima, Y. Honda, O. Kitao, H. Nakai, T. Vreven, J. A., Jr. Montgomery, J. E. Peralta, F. Ogliaro, M. Bearpark, J. J. Heyd, E. Brothers, K. N. Kudin, V. N. Staroverov, R. Kobayashi, J. Normand, K. Raghavachari, A. Rendell, J. C. Burant, S. S. Iyengar, J. Tomasi, M. Cossi, N. Rega, J. M. Millam, M. Klene, J. E. Knox, J. B. Cross, V. Bakken, C. Adamo, J. Jaramillo, R. E. Gomperts, O. Stratmann, A, J. Yazyev, R. Austin, C. Cammi, J. W, Pomelli, R. Ochterski, R. L. Martin, K. Morokuma, V. G. Zakrzewski, G. A. Voth, P. Salvador, J. J. Dannenberg, S. Dapprich, A. D. Daniels, O. Farkas, J. B. Foresman, J. V. Ortiz, J. Cioslowski, D. J. Fox, Gaussian 09, revision A.02; Gaussian, Inc.: Wallingford, CT.

2 A. D. Becke, *The Journal of Chemical Physics*, 1993, **98**, 5648-5652.

3 C. Lee, W. Yang and R. G. Parr, *Physical Review B*, 1988, **37**, 785-789.

4 W. Küchle, M. Dolg, H. Stoll and H. Preuss, *The Journal of Chemical Physics*, 1994, **100**, 7535-7542.

5 X. Cao and M. Dolg, *Journal of Molecular Structure: THEOCHEM*, 2004, **673**, 203-209.

6 X. Cao, M. Dolg and H. Stoll, *The Journal of Chemical Physics*, 2002, **118**, 487-496.

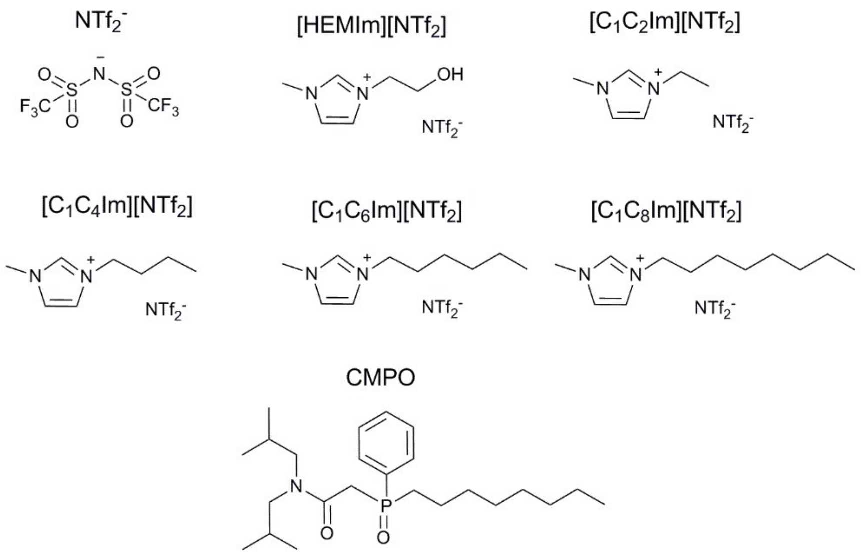

Scheme S1. Structures of ILs and ligand CMPO used in this study.

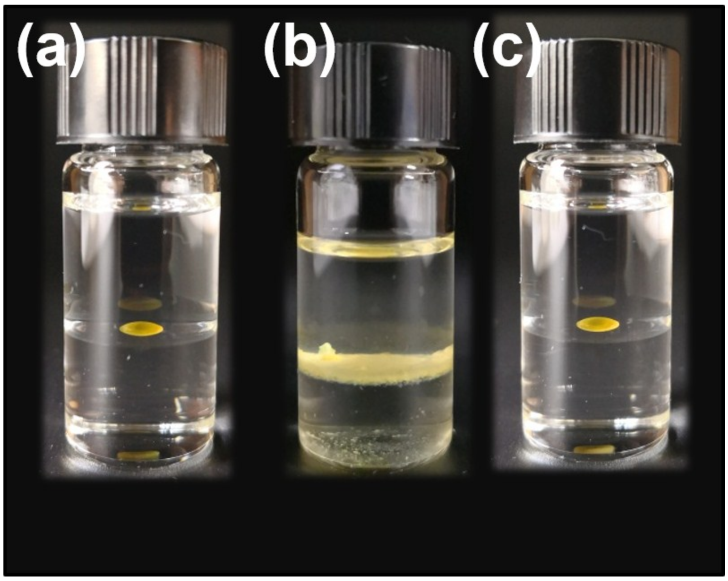

Figure S1. pH-responsive and reversible behavior of the self-assembly process.
(a) Original SA sample is formed with aqueous phase pH=1. (b) SA sample is collapsed after turning the aqueous phase to alkaline environment (pH>14) by adding saturated NaOH solution. (c) Adjustment back to acidic condition (pH=1) and the reappearance of the SA sample.

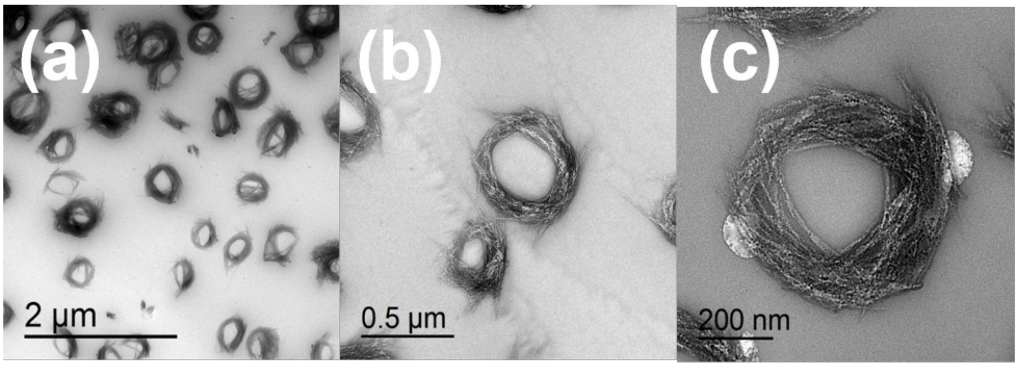

Figure S2. Additional TEM images of the collapsed self-assembly sample with various magnifications.

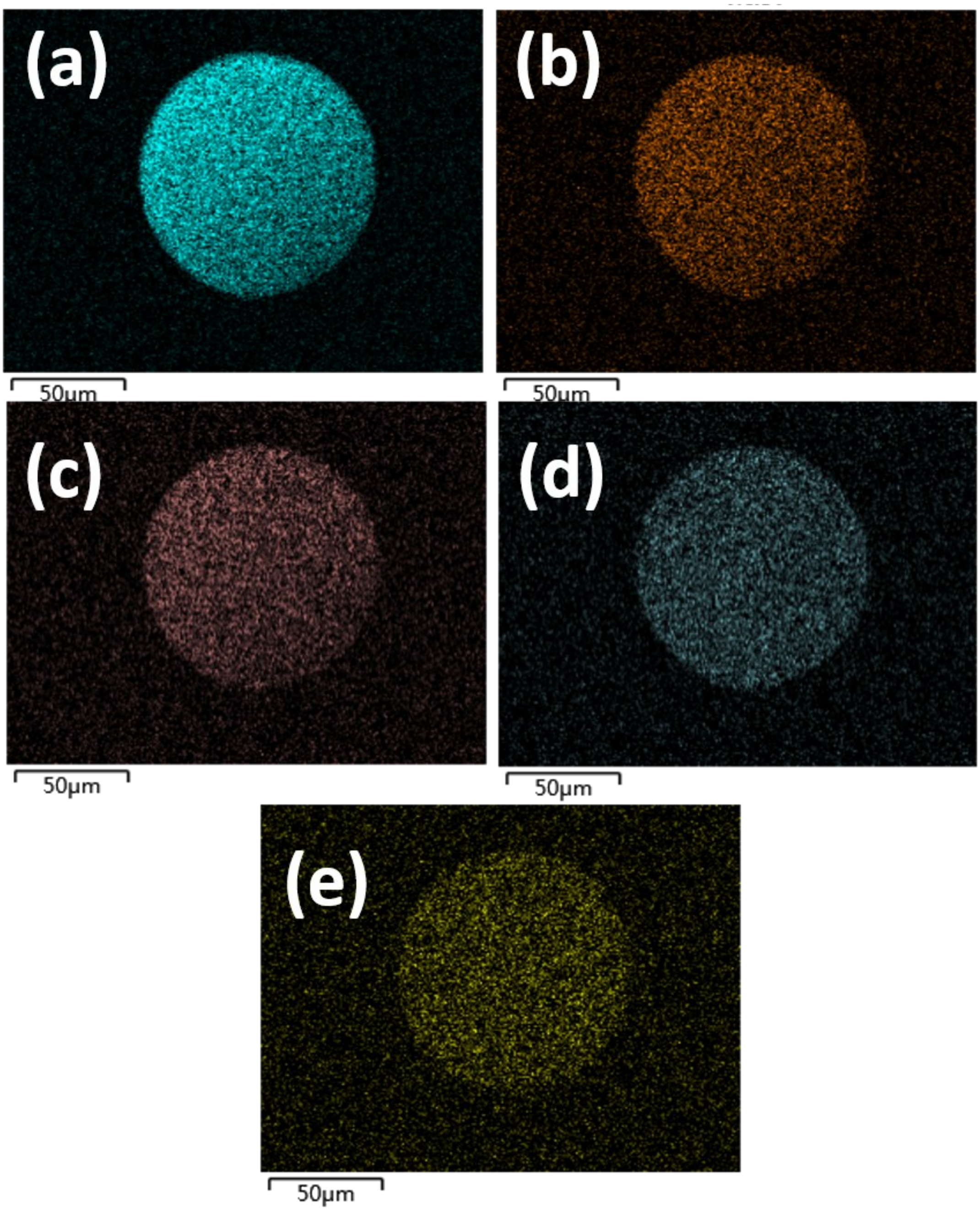

Figure S3. EDS mapping of the self-assembly sample.
(a) carbon, (b) fluorine, (c) oxygen, (d) sulphur, (e) phosphorus.

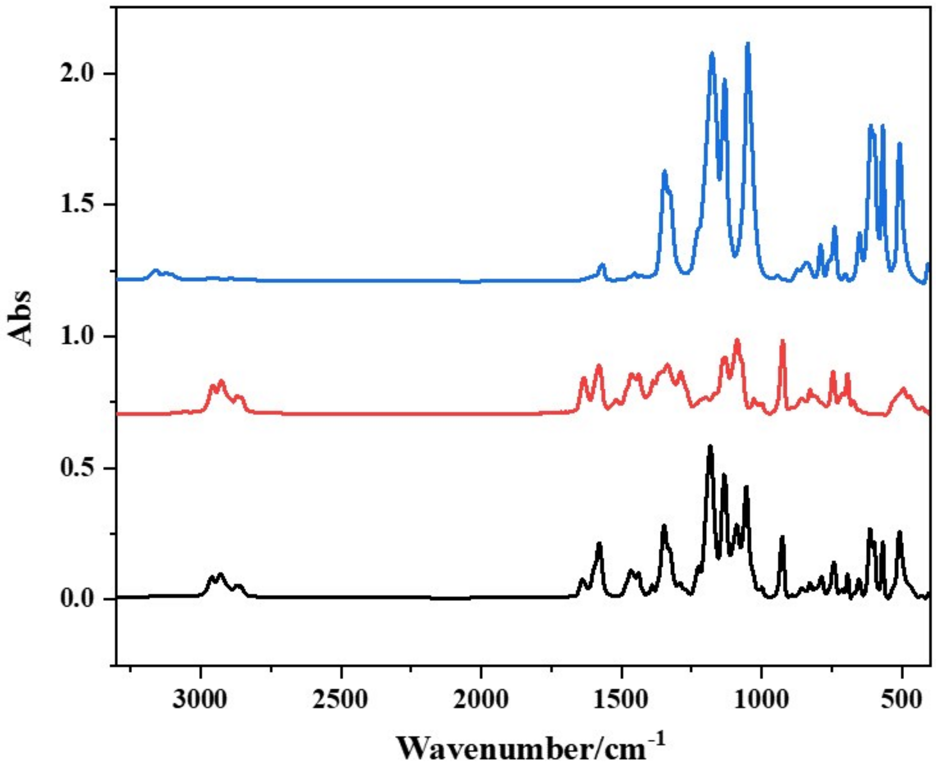

Figure S4. FTIR spectra of [HEMIm][NTf$_2$], UO$_2$(CMPO)$_3$(NO$_3$)$_2$ and the self-assembly sample.

FTIR spectra of [HEMIm][NTf$_2$] (blue curve), UO$_2$(CMPO)$_3$(NO$_3$)$_2$ (red curve) and the self-assembly sample (black curve). No peak at 1338 cm^{-1} (associated with the characteristic absorption of NO$_3^-$) was observed in the IR spectrum of self-assembly sample as compared with that of UO$_2$(CMPO)$_3$(NO$_3$)$_2$, supporting the conclusion of elemental analysis as no existence of NO$_3^-$ in the self-assembly sample.

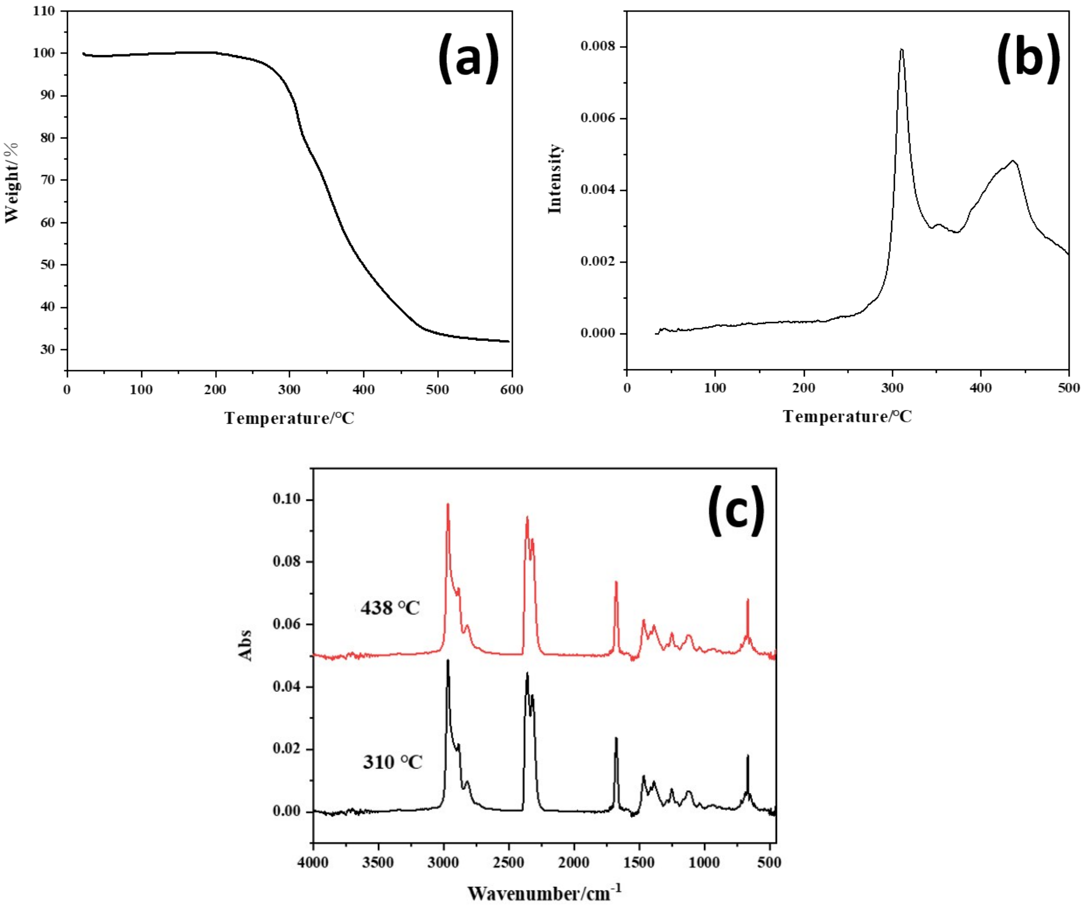

Figure S5. The TGA-FTIR spectra of the self-assembly sample.

(a) TGA curve of the self-assembly sample. No mass loss between 100 and 120 ℃ indicates no water is involved in the supramolecular assembly. (b) Gram-Schmidt curve of the evolved gas. Each point of the curve represents the total intensity of the infrared absorption spectrum of the evolved gas collected at the specific temperature. Two infrared absorption peaks appear at 310 and 438 °C respectively. (c) The corresponding infrared spectra at the peak temperature of the Gram-Schmidt curve. No absorption of gaseous water can be found, suggesting the assembly was not a hydrogel nor containing water molecules.

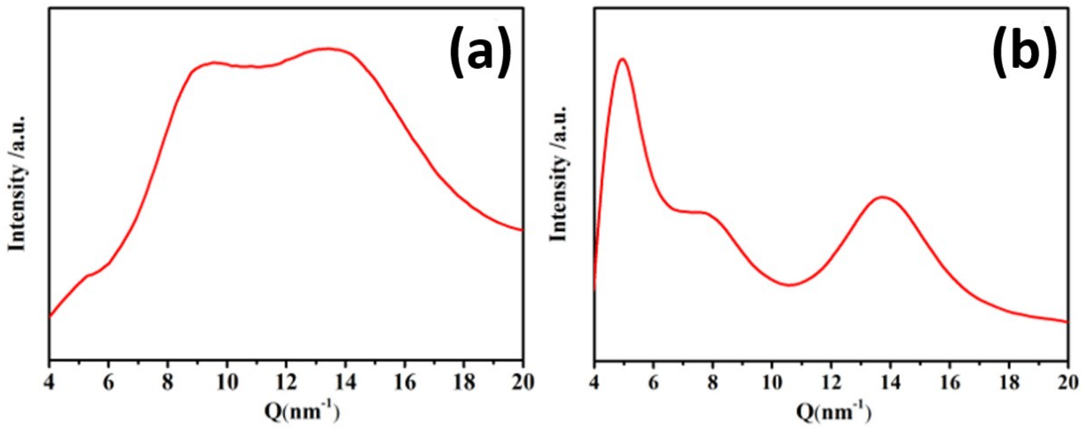

Figure S6. WAXS curves of [HEMIm][NTf$_2$] and self-assembly sample.
(a) [HEMIm][NTf$_2$] (b) self-assembly sample. Two scattering halos could be obtained in the q vs intensity curve of the IL, while the self-assembly sample has a new peak appearing at the center of ~5 nm^{-1}.

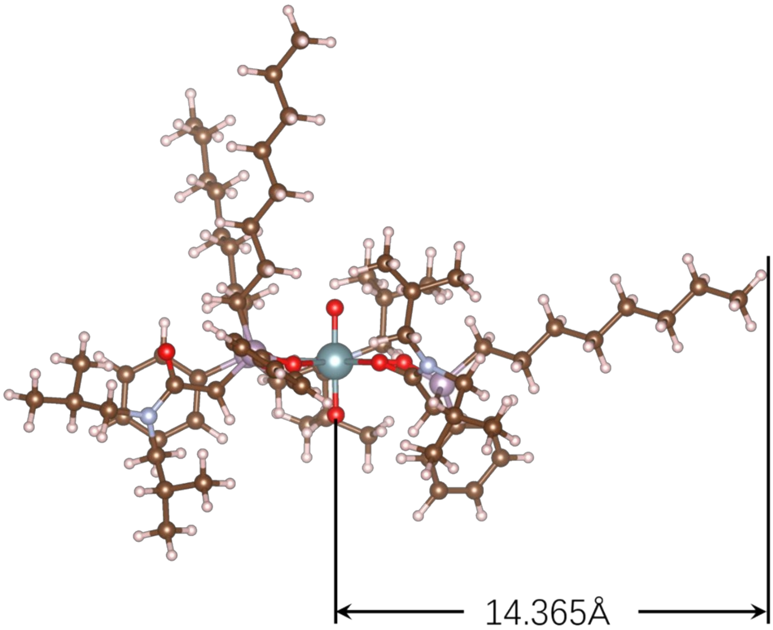

Figure S7. Theorical calculations of the $UO_2(CMPO)_3^{2+}$ complex.

The geometry and corresponding radius parameter of the relaxed lowest energy configuration of the $UO_2(CMPO)_3^{2+}$ complex. The cyan, red, brown, purple, light blue, and white balls represent U, O, C, P, N, and H atoms, respectively.

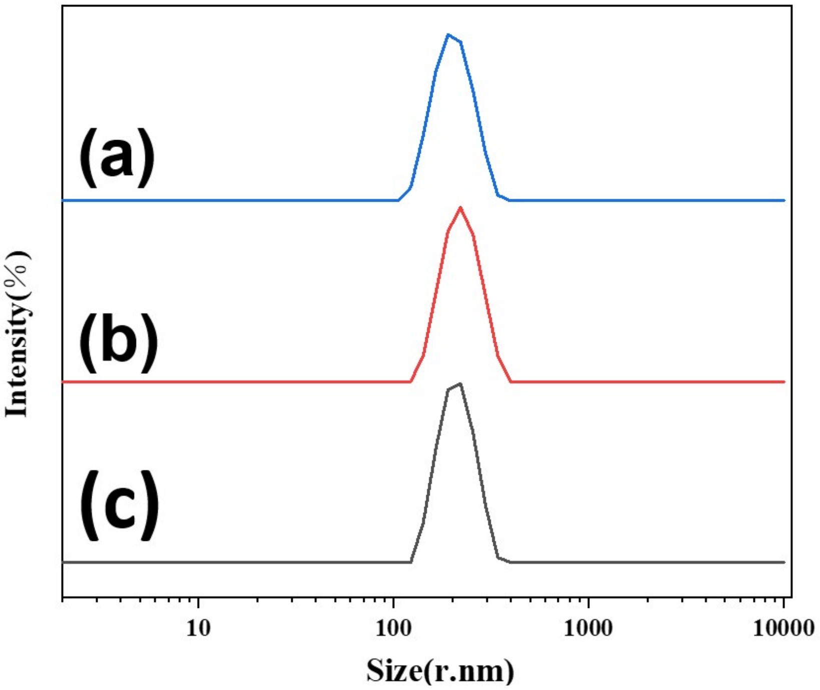

Figure S8. Dynamic light scatting (DLS) results of 3 mL 1 mM $UO_2(CMPO)_3(NTf_2)_2$ in [HEMIm][NTf_2] solutions with different contents of water. (a) 150 μL, (b) 180 μL and (c) 210 μL.

It is difficult to obtain the stable light scattering pattern during the formation procedure of SA sample. The alternative experiment was performed in this work to help to understanding the formation mechanism of SA sample. After adding certain amount of water to the solution of $UO_2(CMPO)_3(NTf_2)_2$ in [HEMIm][NTf_2], it was vortexed to accelerate the dissolution of water. And then, a clear and transparent solution was obtained after centrifugation at 10000 rpm for 10 minutes. After balancing for 2 minutes, the DLS experiment with the excitation wavelength of 633 nm was measured on a Malvern Nano ZS90 instrument (Malvern Instruments, UK) at 30 ℃ and at a scattering angle of 90◦.

There are no DLS signals in all three solutions with [C_1C_2MIm][NTf_2]. Note with the further increase of the water volume, the mixed solution becomes turbid that hinders DLS measurements. In the real events in extraction and formation of the SA sample, the aqueous contents are of comparable volume with IL phase, leading to visible intermediates with larger sizes.

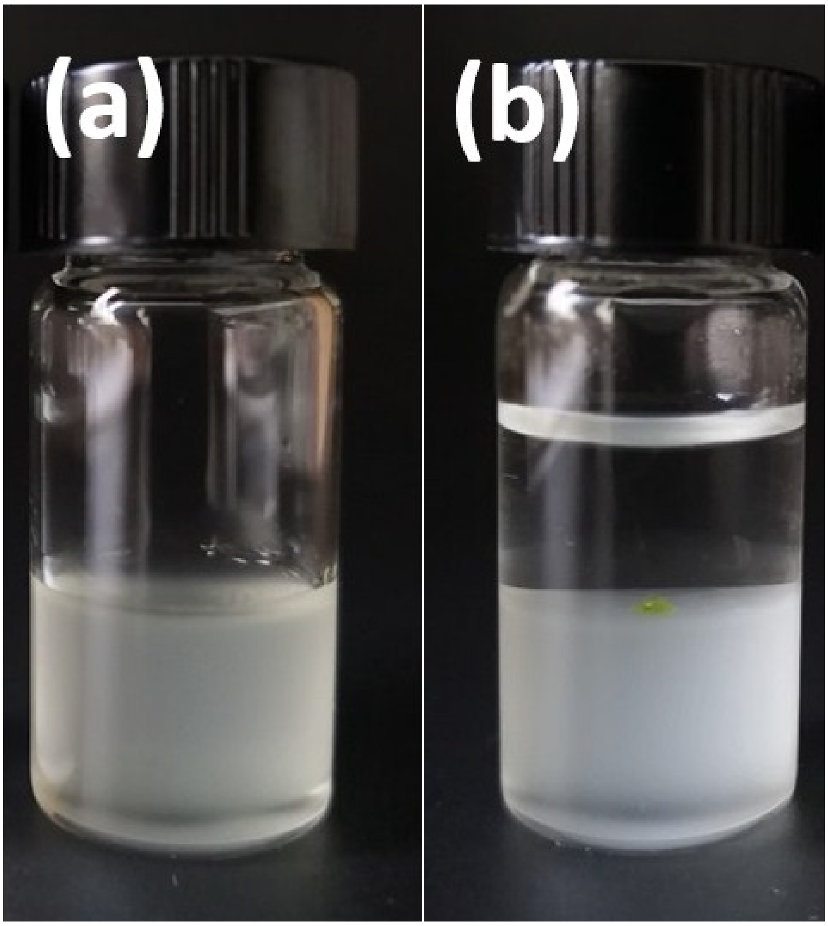

Figure S9. The effect of aqueous-IL interface on the formation of macroscopic SA sample.

(a) Both CMPO and uranyl were dissolved in [HEMIm][NTf$_2$] and mixed to form a turbid liquid. No SA sample was observed. (b) SA sample was formed after addition of 0.1 M HNO$_3$ to form an aqueous-IL interface.

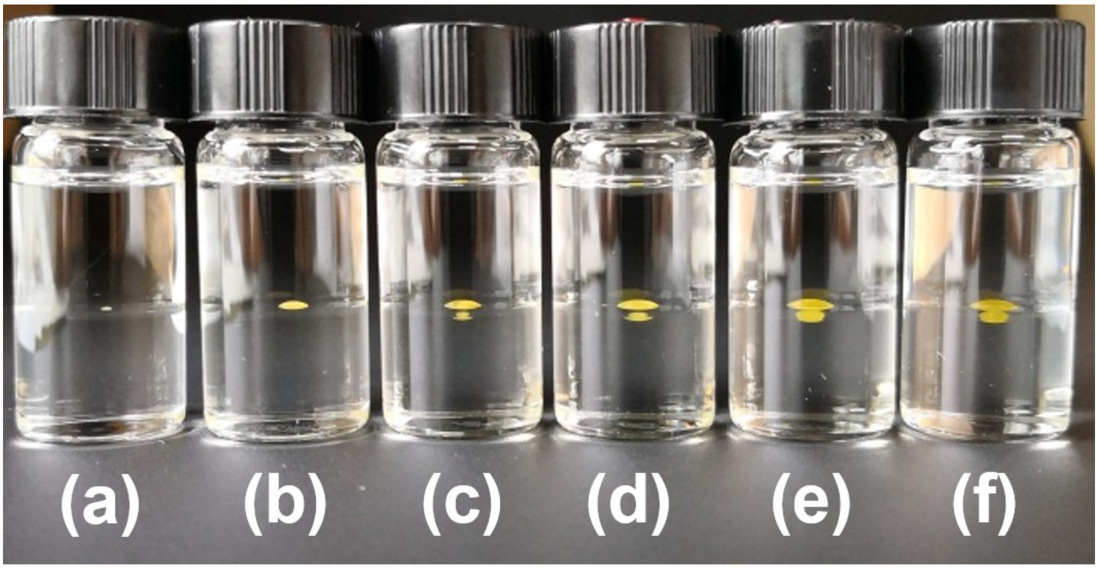

Figure S10. The photographs of uranium-rich SA samples with different ligand/uranyl molar ratios.

(a) 1:1, (b) 2:1, (c) 3:1, (d) 4:1, (e) 5:1, (f) 6:1. As can be seen the size of the SA sample grows concomitantly with the increase of ligand/uranyl ratio from 1:1 to 6:1.

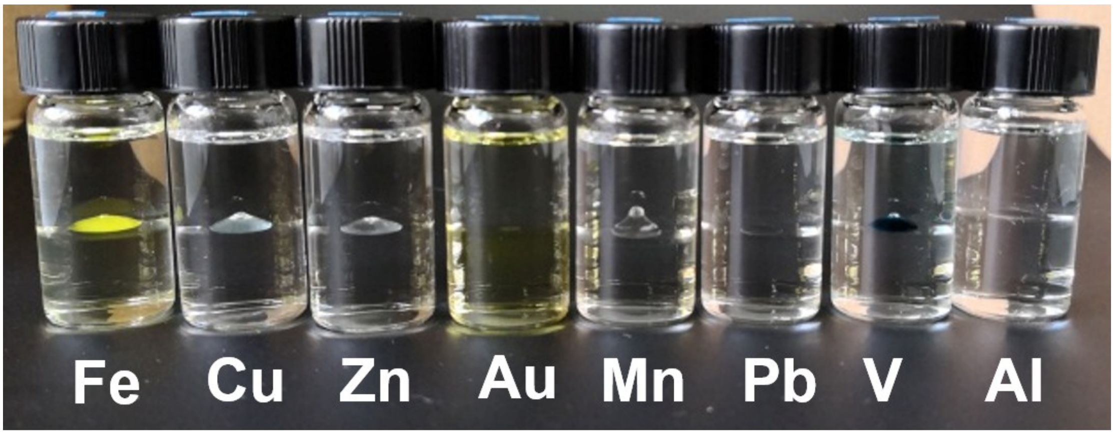

Figure S11. The photographs of visible SA sample formation with various metals. The experimental conditions are similar to that for uranium-rich SA sample formation, but with HCl as the aqueous solvent and different ligand/metal concentration ratio applied.

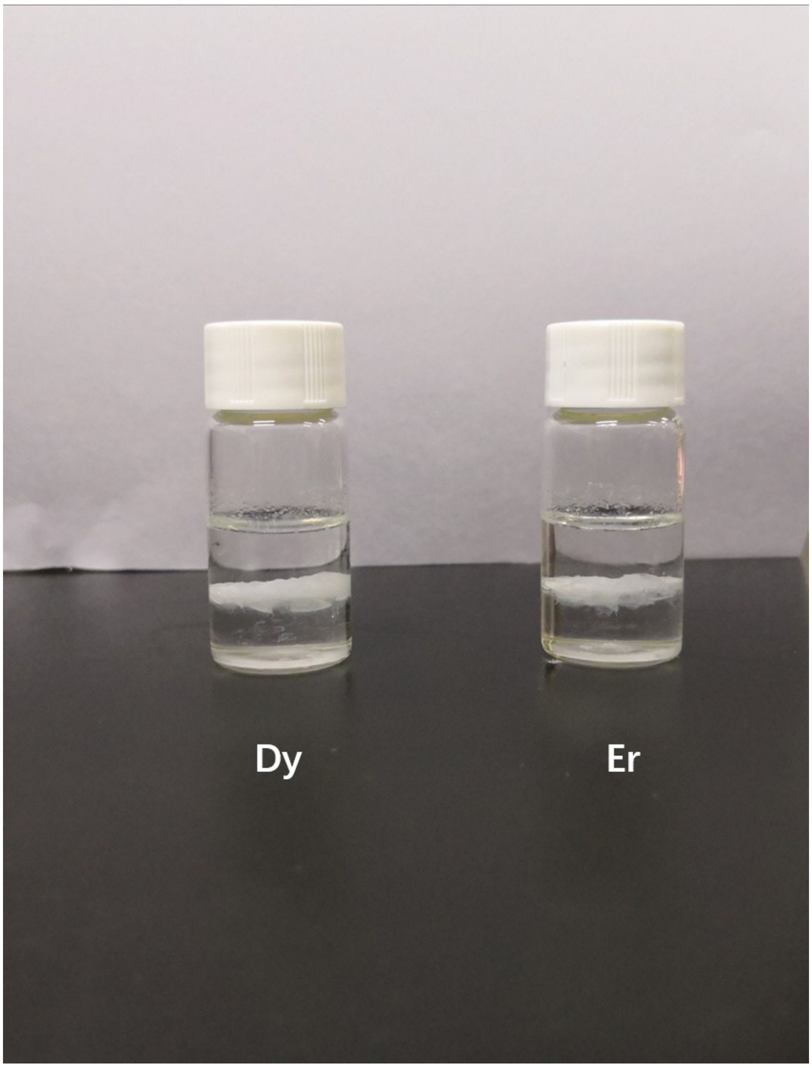

Figure S12. The photographs of the extraction strategy applied to extraction lanthanide ions.

Table S1. Elemental analysis results of the self-assembly sample with different air-drying time

Batch	C/%	H/%	N/%
A	43.33	6.07	3.85
B	43.53	6.05	3.80
C	43.25	6.07	3.89

The SA sample was taken out with a tweezer and placed in a petri dish with an air-drying period of (A) 6 h, (B) 36 h, (C) three weeks. The results are quite close to that of assembly made up of $[UO_2(CMPO)_3]^{2+}$:$[HEMIm]^+$:$[NTf_2]^-$ in a molar ratio of 3:1:7, $C_{236}H_{389}F_{42}N_{18}O_{53}P_9S_{14}U_3$ (Elem. Anal. Calcd (%): C, 43.17; H, 5.97; N, 3.84).

Table S2. Detailed experimental conditions for investigating the effects of CMPO concentration in IL phase and HNO_3 concentration in aqueous phase

Entry	Aqueous phase			IL phase		Notes
	volume	$[UO_2^{2+}]$	$[HNO_3]$	volume	[CMPO]	
	mL	mM	M	mL	mM	
1	2.0	5.0	0.1	2.0	5.0	Effects of CMPO concentration
2	2.0	5.0	0.1	2.0	10.0	
3	2.0	5.0	0.1	2.0	15.0	
4	2.0	5.0	0.1	2.0	20.0	
5	2.0	5.0	0.1	2.0	25.0	
6	2.0	5.0	0.1	2.0	30.0	
7	2.0	5.0	0.1	2.0	35.0	
8	2.0	5.0	0.1	2.0	40.0	
9	2.0	5.0	0.1	2.0	45.0	
10	2.0	5.0	0.1	2.0	50.0	
11	2.0	5.0	0.1	2.0	100.0	
12	2.0	5.0	0.25	2.0	30.0	Effects of HNO_3 concentration
13	2.0	5.0	0.5	2.0	30.0	
14	2.0	5.0	0.75	2.0	30.0	
15	2.0	5.0	1.0	2.0	30.0	
16	2.0	5.0	2.0	2.0	30.0	
17	2.0	5.0	3.0	2.0	30.0	

Table S3. Detailed experimental conditions for investigating the reusability of IL

Cycle	**Aqueous phase**			**IL phase**		**Notes**
	volume	$[UO_2^{2+}]$	$[HNO_3]$	volume	[CMPO]	
	mL	mM	M	mL	mM	
1st	4.0	5.0	0.1	4.0	30.0	
2nd	4.0	5.0	0.1	3.7+0.3	-	3.7 mL recovered IL from 1st cycle and 0.3 mL new IL containing 0.4 M CMPO
3rd	4.0	5.0	0.1	3.7+0.3	-	3.7 mL recovered IL from 2nd cycle and 0.3 mL new IL containing 0.4 M CMPO

Table S4. The loss of ILs in each extraction cycle.

	Loss in the aqueous phase	**Loss in the SA formation**
1st cycle	3.6%	0.31%
2nd cycle	0.87%	0.31%
3rd cycle	0.13%	0.31%

Since ILs could be dissolved in aqueous phase as well participate in the SA formation, both of which could result in the loss of ILs. The amount of ILs lost in aqueous phase was estimated by measuring the concentration of NTf_2^- in the aqueous phase, while the amount of ILs lost in the SA formation could be calculated by the molecular formula of the macroscopic assembly and the content of uranyl ion.

The determination of the concentrations of NTf_2^- in aqueous solutions was performed on a Dionex model ICS-900 ion chromatograph (IC) with Chromeleon 7.0 software (Dionex Corporation, USA). For the analysis of NTf_2^-, an IonPacAS16 analytical column (250 × 4 mm) and an IonPacAG16 guard column (50 × 4 mm) were used. The analytes were eluted by isocratic elution with an aqueous solution of 30 $mmol{\cdot}dm^{-3}$ of KOH and 30% (v/v) acetonitrile at a flow rate of 0.8 $mL{\cdot}min^{-1}$. The suppressor AMMS 300 was installed for chemical suppression with 67 $mmol{\cdot}dm^{-3}$ of H_2SO_4.